

Analyst

Accepted Manuscript



This is an *Accepted Manuscript*, which has been through the Royal Society of Chemistry peer review process and has been accepted for publication.

Accepted Manuscripts are published online shortly after acceptance, before technical editing, formatting and proof reading. Using this free service, authors can make their results available to the community, in citable form, before we publish the edited article. We will replace this *Accepted Manuscript* with the edited and formatted *Advance Article* as soon as it is available.

You can find more information about *Accepted Manuscripts* in the [Information for Authors](#).

Please note that technical editing may introduce minor changes to the text and/or graphics, which may alter content. The journal's standard [Terms & Conditions](#) and the [Ethical guidelines](#) still apply. In no event shall the Royal Society of Chemistry be held responsible for any errors or omissions in this *Accepted Manuscript* or any consequences arising from the use of any information it contains.

1
2
3
4
5
6
7 Solvent-Induced Structural Transitions of
8
9
10
11 Lysozyme in an Electrospray Ionization Source
12
13
14
15

16 *Jong Wha Lee^a and Hugh I. Kim^{a,b,*}*
17

18
19
20 ^aDepartment of Chemistry, and ^bDivision of Advanced Materials Science, Pohang University
21 of Science and Technology (POSTECH), Pohang, 790-784, South Korea
22
23
24
25
26
27
28
29
30
31
32
33
34
35
36
37
38
39
40
41
42
43
44
45
46
47
48
49
50

51
52 *To whom correspondence should be addressed: E-mail: hughkim@postech.edu
53
54
55
56
57
58
59
60

ABSTRACT

The structural characterization of proteins using electrospray ionization mass spectrometry (ESI-MS) has become an important method for understanding protein structural dynamics. The correlation between the structures of proteins in solution and gas phase needs to be understood for the application of ESI-MS to protein structural studies. Hen egg white lysozyme (Lyz) is a small protein with a stable compact structure in solution. Although it was known that denatured Lyz in solution undergoes compaction during transfer into the gas phase *via* ESI, detailed characterization of the process was not available. In the present study, we show that the organic cosolvent, which denatures Lyz in solution, induces the collapse of the extended Lyz structure into compact structures during ESI. This process is further facilitated by the presence of acids, whose conjugate bases can interact with Lyz to reduce its charge state and the electrostatic repulsion between its charged residues (*Analyst* 2015, **140**, 661-669). Exposure of ESI droplets to acid and solvent vapors confirm that the overall process most likely occurs in the charged droplets from ESI. This study provides a detailed understanding of the possible influence of solvent environment on protein structure during transfer into the gas phase.

INTRODUCTION

The recent development of electrospray ionization (ESI)¹ has enabled structural investigations of various proteins using mass spectrometry (MS).² During ESI, charged droplets are initially formed at the tip of a high-voltage capillary, which then undergo cycles of evaporation and fission until molecular ions are produced.³ This process applies significantly small energy to the analyte proteins allowing solution-phase proteins to be transferred intact into the gas phase. Many studies have supported positive correlations between protein structures in solution and the gas phase.⁴⁻¹² For example, unfolding of a protein in solution is reflected by a shift in its charge state distribution (CSD) into higher charge states,^{4,5} and good agreement was observed between protein structural distributions in solution and protein CSDs in ESI-MS spectra.^{6,7} Moreover, the collision cross section (Ω_D) values of proteins, obtained from ion mobility (IM) measurements, are similar to the theoretical Ω_D values of protein crystal structures.^{9, 10} A recent study showed a close relationship between Ω_D and the Stokes radii of proteins and protein complexes.¹¹ Supporting evidence for the preservation of salt bridge structures in the gas phase has also been reported.¹² These reports suggest that the structural aspects of proteins in solution can be maintained after transfer into the gas phase. Utilizing the soft feature of ESI, numerous studies have successfully investigated protein conformations¹³⁻¹⁸ and noncovalent protein assemblies.^{19,20}

The transfer of solution-phase structural information into the gas phase is an important prerequisite for the application of ESI-MS to characterize protein structures. Generally, gentle parameters such as low capillary voltage and low source temperature could aid in preventing protein unfolding during ESI.^{21, 22} However, recent reports show that structural transitions may occur during ESI even under gentle conditions. The unfolding of proteins during ESI can be facilitated by weak acids,²³ low ionic strength,²⁴ buffer decomposition,²⁵

1
2
3
4 and enrichment of other additives.²⁶ In addition, protein structures can also collapse into
5
6 smaller structures during or after transfer into the gas phase.²⁷⁻²⁹ For example, denatured
7
8 myoglobin²⁸ and lysozyme²⁷ can assume compact structures after transfer into the gas phase.
9
10 These examples show that it is important to identify factors that can influence protein
11
12 structure during ESI for more reliable application of ESI-MS to investigate protein structures
13
14 in solution.
15
16

17
18 Douglas and coworkers have previously shown that unfolded lysozyme (Lyz; 14.3 kDa)
19
20 assumes compact structures after transfer into the gas phase.²⁸ Although Lyz is known to be
21
22 present in a helically unfolded conformation in 80% methanol solution at pH 2,³⁰ they were
23
24 unable to observe a shift of the CSD into higher charge states.²⁸ Furthermore, the Ω_D values
25
26 and gas-phase hydrogen-deuterium exchange rates of Lyz ions from the native and denaturing
27
28 solutions were indistinguishable.²⁸ Thus, it was concluded that the Lyz structure collapses
29
30 into compact structures while being transferred into the gas phase, and this was recently
31
32 confirmed by Barran and coworkers.³¹ They reported that Lyz ions with extended
33
34 conformations were not formed from low-pH organic cosolvents.³¹ The intriguing behavior of
35
36 Lyz was interpreted as the refolding of Lyz driven by the four disulfide bonds within the
37
38 protein,^{28, 31} but further mechanistic characterization of this process is yet to be performed.
39
40 While the disulfide bonds seem to be an important factor for the compaction of Lyz during
41
42 ESI, we hypothesize that other factors also contribute to the process. Especially, acids and
43
44 organic solvents used to denature Lyz in solution may actively facilitate the structural
45
46 transition of Lyz during ESI. A more detailed investigation of this process would provide a
47
48 better understanding of how proteins are transferred into the gas phase.
49
50
51

52
53 We have recently shown that acids can induce the structural transition of Lyz from aqueous
54
55 solutions during ESI.²³ It was demonstrated that weak acids, such as formic acid, induce the
56
57 unfolding of Lyz during ESI, whereas the strong acid HCl suppressed unfolding. We inferred
58
59
60

1
2
3
4 that formic acid provided protons to disrupt salt bridges of Lyz, while the addition of HCl
5
6 reduced electrostatic repulsion between charged residues of Lyz because of ion-pairing of
7
8 chloride anions to Lyz.²³ According to this explanation, organic cosolvents should be able to
9
10 facilitate the compaction of proteins during ESI as their intrinsic properties such as low
11
12 surface tension,^{32,33} high gas-phase basicity,³⁴ and promotion of ion-pairing,³⁵ would reduce
13
14 the charge state and the electrostatic repulsion between the charged residues of Lyz. In this
15
16 study, we aimed to reveal the influence of organic solvents on the structure of Lyz ions
17
18 produced using ESI. We performed detailed structural characterization of Lyz in solution
19
20 through circular dichroism (CD) spectroscopy and small-angle X-ray scattering (SAXS)
21
22 experiments. Subsequently, the gas-phase structures of Lyz were investigated based on CSDs
23
24 and IM measurements.
25
26
27

28 **EXPERIMENTAL**

29
30 **Sample Preparation.** Hen egg white Lyz, ammonium acetate, HCl, formic acid, acetic acid,
31
32 ethanol, 1-propanol, and 2-propanol were purchased from Sigma-Aldrich (Saint Louis, MO,
33
34 USA). HPLC-grade water, methanol, and acetonitrile were purchased from Avantor
35
36 Performance Materials, Inc. (Center Valley, PA, USA) and used as solvents. An Orion 3 Star
37
38 pH meter (Thermo Scientific, San Jose, CA, USA) was used to measure the pH of sample
39
40 solutions.
41
42
43

44 **Circular Dichroism (CD) Spectroscopy.** A Jasco J-815 polarimeter (Easton, MD,
45
46 USA) was used at a speed of 50 nm/min and a Lyz concentration of 10 μ M. All
47
48 spectra were averaged from 15 spectra. The formic acid concentration was fixed to 1%
49
50 by volume because higher formic acid concentrations diminished the CD signals. The
51
52 pH values of formic acid solutions are listed in the caption of Figure 1. The samples at
53
54 pH 4.5 and 7 were prepared by adding HCl or ammonia solution.
55
56
57
58
59
60

1
2
3
4 **Small-Angle X-ray Scattering (SAXS).** SAXS experiments were performed at the 4C
5 SAXS II beamline in Pohang Accelerator Laboratory (PAL), with experimental protocols
6 identical to those used in our previous study.²³ Ammonium acetate solutions were prepared
7 by adding acetic acid to 200 mM ammonium acetate solution until the desired pH was
8 obtained. Solvent scattering was subtracted from the sample scattering, and data was
9 analyzed using ATSAS 2.5.2.³⁶⁻³⁹ Radius of gyration (R_g) values of Lyz was estimated using
10 the Guinier relationship (eq. 1).⁴⁰
11
12
13
14
15
16
17
18
19

$$\ln[I(q)] = \ln[I(0)] - R_g^2 q^2 / 3 \quad (1)$$

20
21
22
23 GNOM³⁷ and GASBOR³⁸ were used to obtain *ab initio* structures of Lyz in solution from
24 SAXS curves. The structures were cross-checked with DAMMIN,⁴¹ and good agreement was
25 observed.
26
27
28
29

30 **Electrospray Ionization Ion Mobility Mass Spectrometry (ESI-IM-MS).**

31
32 Experiments were performed with a Waters Synapt G2 HDMS instrument with travelling
33 wave ion mobility spectrometry (TWIMS) capability. Experimental parameters were
34 optimized to ensure that gentle conditions were used. Overall, the parameters were similar to
35 those used in our previous study,²³ with the exception of desolvation gas flow, wave velocity,
36 and wave height, which were 600 L/h, 250 m/s, and 18.0 V, respectively. The calibration of
37 experimental arrival times into Ω_D were performed using previously reported Ω_D values of
38 denatured ubiquitin, cytochrome c, and apomyoglobin.^{41, 42} The IM spectra were smoothed
39 once using the Savitzky-Golay algorithm with one unit of window, using MassLynx 4.1
40 software (Waters, Milford, MA).
41
42
43
44
45
46
47
48
49
50
51

52 **RESULTS AND DISCUSSION**

53
54 **Structure of Lyz in Solution.** The CD spectra in Figure 1a show that the secondary
55 structural change of Lyz is negligible in up to 60% methanol concentration at pH 4.5 and 7.
56
57
58
59
60

1
2
3
4 Lowering the pH to below 3 by adding formic acid and HCl unfolds Lyz in 60% methanol
5 solutions. However, Lyz still maintains its secondary structures in up to 40% methanol
6 concentration under highly acidic conditions, demonstrating its exceptional structural stability.
7
8
9
10 The experimental results are consistent with those of Akasaka and coworkers, which showed
11 that Lyz unfolds in solutions between 40% to 80% methanol depending on the pH.³⁰
12
13
14

15 The tertiary structural information of Lyz provided by the solution SAXS experiments
16 generally agreed with the structural information from the CD spectra (see Figure S1a in the
17 ESI† for raw SAXS profiles). The R_g values of Lyz from Guinier plots of SAXS curves
18 (Figure 1b) are summarized in Table 1. Lyz in water and 40% methanol generally show R_g
19 values of ~ 15.3 Å, which are consistent with the R_g values of native Lyz reported
20 previously.^{23, 30, 39} Slightly smaller R_g values were observed for Lyz in ammonium acetate
21 solutions at pH 4.5, which is inferred to be due to the influence of acetate anions on Lyz (see
22 discussions in the ESI†).⁴³ Kratky plots (Figure 1c) of SAXS curves, which provide overall
23 compactness of the protein, exhibit bell-shaped curves for up to 40% methanol concentration,
24 also demonstrating that Lyz is present as globular structures. At 80% methanol concentration,
25 Lyz undergoes unfolding even under weakly acidic conditions (pH 4.5) and is further
26 unfolded under strongly acidic conditions (pH 2.2), in agreement with the structural
27 information from the CD spectra (Figure 1a). The R_g values of Lyz in these solutions are ~ 22
28 Å, which are approximately 50% greater than the R_g value of native Lyz (Table 1). The *ab*
29 *initio* SAXS envelopes³⁸ for Lyz in Figure 1d (see Figure S1b in the ESI† for theoretical
30 fitting curves) also illustrate that Lyz in 80% methanol solutions has more extended
31 structures than native Lyz. SAXS experiments were unavailable in 80% methanol solution at
32 pH 7 due to the limited solubility of Lyz, but the CD spectra in Figure 1a suggest that Lyz is
33 likely to be unfolded under this condition.
34
35
36
37
38
39
40
41
42
43
44
45
46
47
48
49
50
51
52
53
54
55
56
57
58
59
60

1
2
3
4 The overall experimental results show that the structure of Lyz in solution is greatly
5 dependent on the methanol concentration and pH. No significant dependency of Lyz structure
6 on the use of different acids was observed. Methanol concentrations required to denature Lyz
7 were similar in both HCl and formic acid solutions, and the R_g values of Lyz after unfolding
8 in HCl and formic acid solutions differ by less than 5%. Therefore, it is inferred that
9 dominant factors determining the structural state of Lyz in solution are the electrostatic
10 repulsion between its charged residues (low pH) and hydrophobic interactions (solvent
11 composition).

12
13 **Structure of Lyz after Transfer into the Gas Phase.** The MS spectrum of Lyz in water in
14 Figure 2 is centered at +10 charge state, in agreement with the previously reported CSDs of
15 Lyz.^{8, 23, 28, 44} The CSD of Lyz from 80% methanol solution is highly similar to that from
16 water, which indicates that CSDs are unable to describe the structural transition of Lyz in
17 solution. Furthermore, while addition of acids further unfolds Lyz in 80% methanol solutions,
18 the CSDs at pH 2.2 are shifted to lower charge states rather than to higher charge states.
19 Unfolding of a protein generally enlarges its solvent accessible surface area and increases its
20 charge states.^{5, 45} ~50% increase in the R_g value of Lyz in 80% methanol solutions (Table 1)
21 approximately corresponds to ~125% increase in its surface area. Therefore, the absence of
22 charge shifts suggests that unfolded Lyz contracts into compact structures during transfer into
23 the gas phase, before charging occurs.

24
25 In order to understand the correlation between structures of Lyz in solution and the
26 gas phase, Ω_D distributions of Lyz from different solutions were compared. A detailed
27 structural characterization of Lyz ions in the gas phase was performed in our previous
28 study.²³ Briefly, we classified structures of Lyz ions in the gas phase into three distinct
29 classes (A, B, and C) depending on their trends in charge- Ω_D correlations (see Figure
30 4a in ref 23). +6 and +7 charged Lyz ions have compact conformations that resemble
31
32
33
34
35
36
37
38
39
40
41
42
43
44
45
46
47
48
49
50
51
52
53
54
55
56
57
58
59
60

1
2
3
4 the compact native state structure, and are classified as A class ions ($\Omega_D = 1320 \sim$
5 1390 \AA^2). B class ions with greater Ω_D are observed at higher charge states (+8 to +12),
6 and their Ω_D increases with increasing charge states ($\Omega_D = 1750 \sim 2150 \text{ \AA}^2$). Addition
7 of weak acids unfolds Lyz during ESI to facilitate the formation of B class ions at low
8 charge states (+6 and +7) with Ω_D greater than those of the A class ions, and C class
9 ions with very large Ω_D at high charge states (+10 to +12; $\Omega_D = 2370 \sim 2510 \text{ \AA}^2$).
10 Figure 3 compares the Ω_D distributions of Lyz from 80% methanol solutions (black
11 solid lines) and pure water (red dots). For Lyz ions from the two different solutions, A
12 class ions dominates at low charge states (+6 and +7) and B class ions dominate higher
13 charge states (+8 to +12) with no signature of C class ions. Analogously to the CSDs,
14 the Ω_D distributions of Lyz ions from 80% methanol solutions are similar with those of
15 Lyz ions from pure aqueous solution. These observations suggest that Lyz does not
16 maintain its solution-phase structural information after transfer into the gas phase.
17
18
19
20
21
22
23
24
25
26
27
28
29
30
31

32
33 Figure 3 shows that Lyz ions from the formic acid solution exhibit extra
34 distributions with greater Ω_D at +6 and +12 charge states, in comparison with those
35 from pure water. However, this result should be compared with the Ω_D distributions of
36 Lyz from aqueous formic acid solution (see Figure 3 in ref 23 for IM spectra), because
37 the addition of formic acid causes more unfolded Lyz ions to be formed during ESI.²³
38 Figure 4 illustrates that ions from 80% methanol/formic acid solution are relatively
39 smaller in size than ions formed from aqueous formic acid solution by formic acid-
40 induced unfolding.²³ Especially, the Ω_D of B class ions observed at +6 charge state is
41 reduced (from 1495 \AA^2 to 1434 \AA^2), and the C class ions observed at +10 to +12
42 charge states disappear. Although not all different peaks can be completely resolved
43 due to the low resolution of the IMS technique, these data were reproducible over
44 three experiments and 9 months of time span.
45
46
47
48
49
50
51
52
53
54
55
56
57
58
59
60

1
2
3
4 The observation of smaller ions from methanol cosolvent is notable as it suggests
5 that methanol is suppressing the formation of extended Lyz ions, which is a reversed
6 effect of methanol in solution. Therefore, compaction of unfolded Lyz during transfer
7 into the gas phase is not only due to the intrinsic properties of Lyz, but is also
8 facilitated by the presence of the organic solvent used to denature the protein in
9 solution. Formic acid-induced unfolding is also suppressed in 40% methanol solution
10 (Figures S2 and S3 in the ESI†), but the ions formed are generally greater in size than
11 those formed from 80% methanol solutions. As methanol unfolds Lyz in solution, this
12 observation also supports the contention that methanol suppresses the formation of
13 unfolded Lyz ions. Further evidence for the effect of methanol is given by the
14 suppression of acetic acid-induced unfolding²³ in both 40% and 80% methanol
15 solutions (see Figure S5 and discussions in the ESI†).

16
17
18
19
20
21
22
23
24
25
26
27
28
29
30
31 **Vapor Exposure of Lyz during ESI and Other Organic Solvent Effects.** For more
32 detailed characterization of structural transitions of Lyz during ESI, vapor exposure
33 experiments⁴⁶⁻⁴⁸ were employed. Vapor exposure of ESI droplets can induce folding or
34 refolding of proteins within,^{46, 47} and this experimental procedure would decouple
35 possible solution-phase conformational effects on gas-phase Lyz structures. For the
36 following series of experiments, the vapor was produced by placing a glass vial
37 containing formic acid or methanol in the ESI chamber,⁴⁸ and Lyz was subjected to
38 ESI in the presence of the vapor.

39
40
41
42
43
44
45
46
47
48
49
50
51
52
53
54
55
56
57
58
59
60
Regardless of solution compositions, exposure to formic acid or methanol vapor during ESI shifted the CSD of Lyz to lower states centered at +8 charge state (Figure S6 in the ESI†). This again suggests that the structural information of Lyz in solution does not remain in the CSDs. The IM distributions of Lyz ions formed in the presence (black lines) and the absence (red dots) of vapor show how structural transitions of

1
2
3
4 Lyz occur during ESI (Figure 5). Firstly, exposure of Lyz in water to formic acid
5 vapor caused unfolded Lyz ions (B class ions; $\Omega_D = 1466 \text{ \AA}^2$) to be observed at the +6
6 charge state, showing that formic acid-induced unfolding occurs during ESI (Figure
7 5a). When Lyz is in 80% methanol solution, the abundance of the unfolded Lyz ion is
8 reduced, demonstrating that methanol can reduce unfolding of Lyz during ESI (Figure
9 5b). It is further observed that methanol exposure also decreases abundance of the
10 unfolded conformers formed by formic acid-induced unfolding ($\Omega_D = 1491$ and 1432
11 \AA^2 , Figures 5c and 5d, respectively). These series of experiments show that the
12 structural transition of Lyz indeed occurs during ESI, and that methanol can actively
13 participate in the contraction of the Lyz structure during the ionization process.
14
15

16
17 To test the generality of solvent effect on the Lyz structure during ESI, further
18 experiments were performed with other organic cosolvents (80% acetonitrile, ethanol,
19 and 1-propanol) containing formic acid. It was observed that addition of these solvents
20 also shift the CSDs into lower charge states (Figure 6a) and reduce the size or
21 abundance B class ions at +6 charge state (Figure 6b). These results indicate that
22 suppression of Lyz unfolding is facilitated by properties that are commonly shared by
23 different organic solvents.
24
25

26
27 **Influence of Organic Solvents on Lyz during Transfer into the Gas Phase.** Our
28 experimental results show that both the addition of methanol to the ESI solution and exposure
29 of aqueous ESI droplets to methanol vapor promoted compaction of Lyz during ESI. As
30 organic solvents may operate in a different manner during these two processes, they require
31 separate discussion. We first discuss the case where methanol was added directly to the ESI
32 solution. The charged residue model (CRM)^{3,49} predicts that low surface tension of organic
33 solvents reduces the charge density of ESI droplets, and thus reduces the charge state of
34 protein ions.³² On the contrary, others discuss that protein charge states do not strictly follow
35
36
37
38
39
40
41
42
43
44
45
46
47
48
49
50
51
52
53
54
55
56
57
58
59
60

1
2
3
4 the surface tension of the solvent used.^{8, 50, 51} Some explanation for conflicting interpretations
5
6 on the role of solvent properties during ESI may come from the preferential evaporation of
7
8 more volatile components.³³ Our experimental results show that both CSDs and IM
9
10 distributions of Lyz from 40% (Figures S2 and S3 in the ESI†) and 80% methanol solution
11
12 (Figures 2 and 3) are highly similar with those from pure aqueous solution (Figures 2 and 3).
13
14 These results suggest that methanol is depleted preferentially from charged droplets
15
16 generated with ESI, and has a limited influence at the later stages of ESI where desolvated
17
18 protein ions are formed.
19
20

21
22 However, additional explanation is required because the influence of methanol is
23
24 significant in acidic solutions. The CSDs of Lyz from methanol solutions at low pH (Figure
25
26 2) are generally centered at lower charge states in comparison to those we reported from
27
28 aqueous solutions at low pH.²³ It was also observed that methanol reduces the size or
29
30 abundance of more unfolded conformers in a given charge state (Figure 3), which indicates
31
32 that the solvent effect can persist in charged droplets containing acids. We have previously
33
34 reported that the acid effect persists to the later stages of ionization because acids protonate
35
36 protein residues and induce protein unfolding or reduce protein charge states by adduction of
37
38 acid anions.²³ This explains why the effect of organic solvents is particularly significant
39
40 under acidic conditions. Although methanol evaporates preferentially over water, the low
41
42 dielectric constant of methanol could facilitate acid anion binding to Lyz during ESI.³⁵ This
43
44 effect may later be reflected in the CSDs as acid anions can abstract protein charges.⁵²
45
46 Stabilization of compact conformers (A class ions at low charge states and B class ions at
47
48 higher charge states) by methanol can be interpreted with reduction in the electrostatic
49
50 repulsion between charged residues of Lyz following acid anion binding.²³ Additionally, a
51
52 decrease in the methanol content during ESI would also facilitate the structural collapse of
53
54 Lyz, as water would relatively be enriched. The explanation based on ion-pairing also
55
56
57
58
59
60

1
2
3
4 rationalizes the observation that the MS and IM spectra of Lyz in acetonitrile solution
5
6 (Figures S6 and 6) are most similar with those of Lyz in methanol solution (Figures 2 and 3).
7
8 Notably, the dielectric constants of methanol (33.0) and acetonitrile (36.64) are highly
9
10 similar, whereas other properties such as gas-phase basicity, vapor pressure, surface tension,
11
12 boiling point, and viscosity are either significantly different or also similar with those of other
13
14 organic solvents (see Table S1 in the ESI†). This supports that ion association and
15
16 dissociation phenomenon have significant effects on the formation of Lyz ions.
17
18

19
20 A very recent report by DeMuth and McLuckey has shown that exposure of ESI droplets to
21
22 organic vapors can reduce metal adduction to protein ions.⁵³ They discussed that organic
23
24 solvents inside charged droplets can lower the barrier for ion evaporation of metal cations,
25
26 and this argument was supported by intense signals of metal-organic solvent clusters
27
28 observed at low m/z .⁵³ The proposed mechanism can rationalize why methanol vapor
29
30 prevented the formation of unfolded ions during ESI, because ion evaporation of protons
31
32 facilitated by methanol vapor would reduce the proton density within the ESI droplets.
33
34 Consequently, the proton concentration available for Lyz would decrease, and anions would
35
36 be relatively enriched to decrease the overall charge state of Lyz during ESI. It is also
37
38 possible that further charge reduction by methanol, which is more basic than water, affects
39
40 the charge state of Lyz after desolvation in the gas phase. However, our vapor exposure
41
42 experiments (Figure 5) show that the solvent effect is mostly operative in the charged droplet.
43
44 Overall, the structural transition of Lyz from an unfolded state in solution to a compact
45
46 structure in the gas phase during ESI is facilitated by charge reduction of Lyz by organic
47
48 solvents.
49
50

51 52 53 **CONCLUSION**

54
55 Although the peculiar properties of Lyz during transfer into the gas phase have long
56
57 been known, detailed investigation of the process was not available. We have shown
58
59
60

1
2
3
4 that methanol and acids cooperate to facilitate the structural transition, during ESI, of
5
6 Lyz from an unfolded state in solution to compact structures in the gas phase. This
7
8 study provides additional insights into the influence of organic solvents on the charge
9
10 state and structural distribution of protein ions formed using ESI, which is currently
11
12 not completely understood. Although the low surface tension of organic solvents has
13
14 received the most attention, our study shows that the low dielectric properties of
15
16 organic solvents could exert additional effects on proteins during transfer into the gas
17
18 phase. Additionally, our detailed characterization of Lyz indicates that its structure in
19
20 the gas phase is most dependent on the ionization process; therefore, Lyz may be used
21
22 to reveal other potential factors influencing protein structures during ESI.
23
24

25 26 **ACKNOWLEDGEMENTS**

27
28 This work was supported by a Basic Research Program (grant no.
29
30 2013R1A1A2008974) through the National Research Foundation (NRF) of Korea
31
32 funded by the Ministry of Science, ICT, and Future Planning (MSIP) and a grant of
33
34 the Korea Health Technology R&D Project through the Korea Health Industry
35
36 Development Institute (KHIDI), funded by the Ministry of Health & Welfare of Korea
37
38 (grant no. HT13C-0011-040013).
39
40

41 42 **NOTES AND REFERENCES**

43
44 ^a Department of Chemistry, Pohang University of Science and Technology, Pohang, 790-
45
46 784, South Korea

47
48 ^b Division of Advanced Materials Science, Pohang University of Science and
49
50 Technology, Pohang, 790-784, South Korea. E-mail: hughkim@postech.edu; Tel: +82-
51
52 54-279-2341

53
54
55 † Electronic Supplementary Information (ESI) available: Additional discussions and
56
57 additional data (Figures S1 – S6 and Table S1) are included. See DOI: 10.1039/b000000x/
58
59
60

1. J. Fenn, M. Mann, C. Meng, S. Wong and C. Whitehouse, *Science*, 1989, **246**, 64-71.
2. R. H. H. v. d. Heuvel and A. J. R. Heck, *Curr. Opin. Chem. Biol.*, 2004, **8**, 519-526.
3. L. Konermann, E. Ahadi, A. D. Rodriguez and S. Vahidi, *Anal. Chem.*, 2013, **85**, 2-9.
4. Z. Hall and C. V. Robinson, *J. Am. Soc. Mass Spectrom.*, 2012, **23**, 1161-1168.
5. L. Testa, S. Brocca and R. Grandori, *Anal. Chem.*, 2011, **83**, 6459-6463.
6. L. Konermann, B. A. Collings and D. J. Douglas, *Biochemistry*, 1997, **36**, 5554-5559.
7. A. Dobo and I. A. Kaltashov, *Anal. Chem.*, 2001, **73**, 4763-4773.
8. M. Šamalíková, I. Matecko, N. Muller and R. Grandori, *Anal. Bioanal. Chem.*, 2004, **378**, 1112-1123.
9. T. Wyttenbach and M. T. Bowers, *J. Phys. Chem. B*, 2011, **115**, 12266-12275.
10. D. E. Clemmer, R. R. Hudgins and M. F. Jarrold, *J. Am. Chem. Soc.*, 1995, **117**, 10141-10142.
11. D. Hewitt, E. Marklund, D. J. Scott, C. V. Robinson and A. J. Borysik, *J. Phys. Chem. B*, 2014, **118**, 8489-8495.
12. Z. Zhang, S. Browne and R. Vachet, *J. Am. Soc. Mass Spectrom.*, 2014, **25**, 604-613.
13. S. W. Heo, T. S. Choi, K. M. Park, Y. H. Ko, S. B. Kim, K. Kim and H. I. Kim, *Anal. Chem.*, 2011, **83**, 7916-7923.
14. J. A. Loo, R. R. O. Loo, H. R. Udseth, C. G. Edmonds and R. D. Smith, *Rapid Commun. Mass Spectrom.*, 1991, **5**, 101-105.
15. U. A. Mirza, S. L. Cohen and B. T. Chait, *Anal. Chem.*, 1993, **65**, 1-6.
16. J. W. Lee, S. W. Heo, S. J. C. Lee, J. Y. Ko, H. Kim and H. I. Kim, *J. Am. Soc. Mass Spectrom.*, 2013, **24**, 21-29.
17. S. J. C. Lee, J. W. Lee, T. S. Choi, K. S. Jin, S. Lee, C. Ban and H. I. Kim, *Anal. Chem.*, 2014, **86**, 1909-1916.
18. A. Litwińczuk, S. R. Ryu, L. A. Nafie, J. W. Lee, H. I. Kim, Y. M. Jung and B. Czarnik-Matuszewicz, *BBA-Proteins Proteom.*, 2014, **1844**, 593-606.
19. M. Sharon and C. V. Robinson, *Annu. Rev. Biochem.*, 2007, **76**, 167-193.
20. A. J. R. Heck, *Nat. Methods*, 2008, **5**, 927-933.
21. H. J. Sterling, C. A. Cassou, A. C. Susa and E. R. Williams, *Anal. Chem.*, 2012, **84**, 3795-3801.
22. U. A. Mirza and B. T. Chait, *Int. J. Mass Spectrom. Ion Processes*, 1997, **162**, 173-181.
23. J. W. Lee and H. I. Kim, *Analyst*, 2015, **140**, 661-669.
24. H. Lin, E. N. Kitova, M. A. Johnson, L. Eugenio, K. K. S. Ng and J. S. Klassen, *J. Am. Soc. Mass Spectrom.*, 2012, **23**, 2122-2131.
25. J. B. Hedges, S. Vahidi, X. Yue and L. Konermann, *Anal. Chem.*, 2013, **85**, 6469-6476.
26. H. J. Sterling, J. S. Prell, C. A. Cassou and E. R. Williams, *J. Am. Soc. Mass Spectrom.*, 2011, **22**, 1178-1186.
27. H. Sterling, M. Daly, G. Feld, K. Thoren, A. Kintzer, B. Krantz and E. Williams, *J. Am. Soc. Mass Spectrom.*, 2010, **21**, 1762-1774.
28. D. M. Mao, K. R. Babu, Y. L. Chen and D. J. Douglas, *Anal. Chem.*, 2003, **75**, 1325-1330.
29. K. Pagel, E. Natan, Z. Hall, A. R. Fersht and C. V. Robinson, *Angew. Chem. Int. Ed.*, 2013, **52**, 361-365.
30. Y. O. Kamatari, T. Konno, M. Kataoka and K. Akasaka, *Protein Sci.*, 1998, **7**, 681-688.

- 1
- 2
- 3
- 4 31. R. Beveridge, S. Covill, K. J. Pacholarz, J. M. D. Kalapothakis, C. E. MacPhee and P.
- 5 E. Barran, *Anal. Chem.*, 2014, **86**, 10979-10991.
- 6 32. A. T. Iavarone and E. R. Williams, *J. Am. Chem. Soc.*, 2003, **125**, 2319-2327.
- 7 33. R. L. Grimm and J. L. Beauchamp, *J. Phys. Chem. A*, 2010, **114**, 1411-1419.
- 8 34. A. Iavarone, J. Jurchen and E. Williams, *J. Am. Soc. Mass Spectrom.*, 2000, **11**, 976-
- 9 985.
- 10 35. G. Wang and R. Colecor, *J. Am. Soc. Mass Spectrom.*, 1996, **7**, 1050-1058.
- 11 36. P. V. Konarev, V. V. Volkov, A. V. Sokolova, M. H. J. Koch and D. I. Svergun, *J.*
- 12 *Appl. Crystallogr.*, 2003, **36**, 1277-1282.
- 13 37. D. Svergun, *J. Appl. Crystallogr.*, 1992, **25**, 495-503.
- 14 38. D. I. Svergun, M. V. Petoukhov and M. H. J. Koch, *Biophys. J.*, 2001, **80**, 2946-2953.
- 15 39. D. Svergun, C. Barberato and M. H. J. Koch, *J. Appl. Crystallogr.*, 1995, **28**, 768-773.
- 16 40. C. D. Putnam, M. Hammel, G. L. Hura and J. A. Tainer, *Q. Rev. Biophys.*, 2007, **40**,
- 17 191-285.
- 18 41. B. T. Ruotolo, J. L. P. Benesch, A. M. Sandercock, S.-J. Hyung and C. V. Robinson,
- 19 *Nat. Protocols*, 2008, **3**, 1139-1152.
- 20 42. M. F. Bush, Z. Hall, K. Giles, J. Hoyes, C. V. Robinson and B. T. Ruotolo, *Anal.*
- 21 *Chem.*, 2010, **82**, 9557-9565.
- 22 43. A. Ducruix, J. P. Guilloteau, M. Riès-Kautt and A. Tardieu, *J. Cryst. Growth*, 1996,
- 23 **168**, 28-39.
- 24 44. M. I. Catalina, R. H. H. van den Heuvel, E. van Duijn and A. J. R. Heck, *Chem. Eur.*
- 25 *J.*, 2005, **11**, 960-968.
- 26 45. L. Konermann, *J. Phys. Chem. B*, 2007, **111**, 6534-6543.
- 27 46. A. Kharlamova, B. M. Prentice, T.-Y. Huang and S. A. McLuckey, *Anal. Chem.*,
- 28 2010, **82**, 7422-7429.
- 29 47. A. Kharlamova, J. C. DeMuth and S. McLuckey, *J. Am. Soc. Mass Spectrom.*, 2012,
- 30 **23**, 88-101.
- 31 48. K. Sokratous, L. V. Roach, D. Channing, J. Strachan, J. Long, M. S. Searle, R.
- 32 Layfield and N. J. Oldham, *J. Am. Chem. Soc.*, 2012, **134**, 6416-6424.
- 33 49. J. Fernandez de la Mora, *Anal. Chim. Acta*, 2000, **406**, 93-104.
- 34 50. M. Šamalikova and R. Grandori, *J. Am. Chem. Soc.*, 2003, **125**, 13352-13353.
- 35 51. M. Šamalikova and R. Grandori, *J. Mass Spectrom.*, 2005, **40**, 503-510.
- 36 52. U. A. Mirza and B. T. Chait, *Anal. Chem.*, 1994, **66**, 2898-2904.
- 37 53. J. C. DeMuth and S. A. McLuckey, *Anal. Chem.*, 2015, **87**, 1210-1218.
- 38
- 39
- 40
- 41
- 42
- 43
- 44
- 45
- 46
- 47
- 48
- 49
- 50
- 51
- 52
- 53
- 54
- 55
- 56
- 57
- 58
- 59
- 60

Figure 1. a) CD spectra of Lyz at different pH and methanol (MeOH) concentrations. The pH values of formic acid solutions are 2.2, 2.3, 2.8, and 2.8 for 0, 40, 60, and 80% methanol solutions, respectively. b) Guinier plots, c) Kratky plots, d) *ab initio* envelopes of Lyz from SAXS experiments.

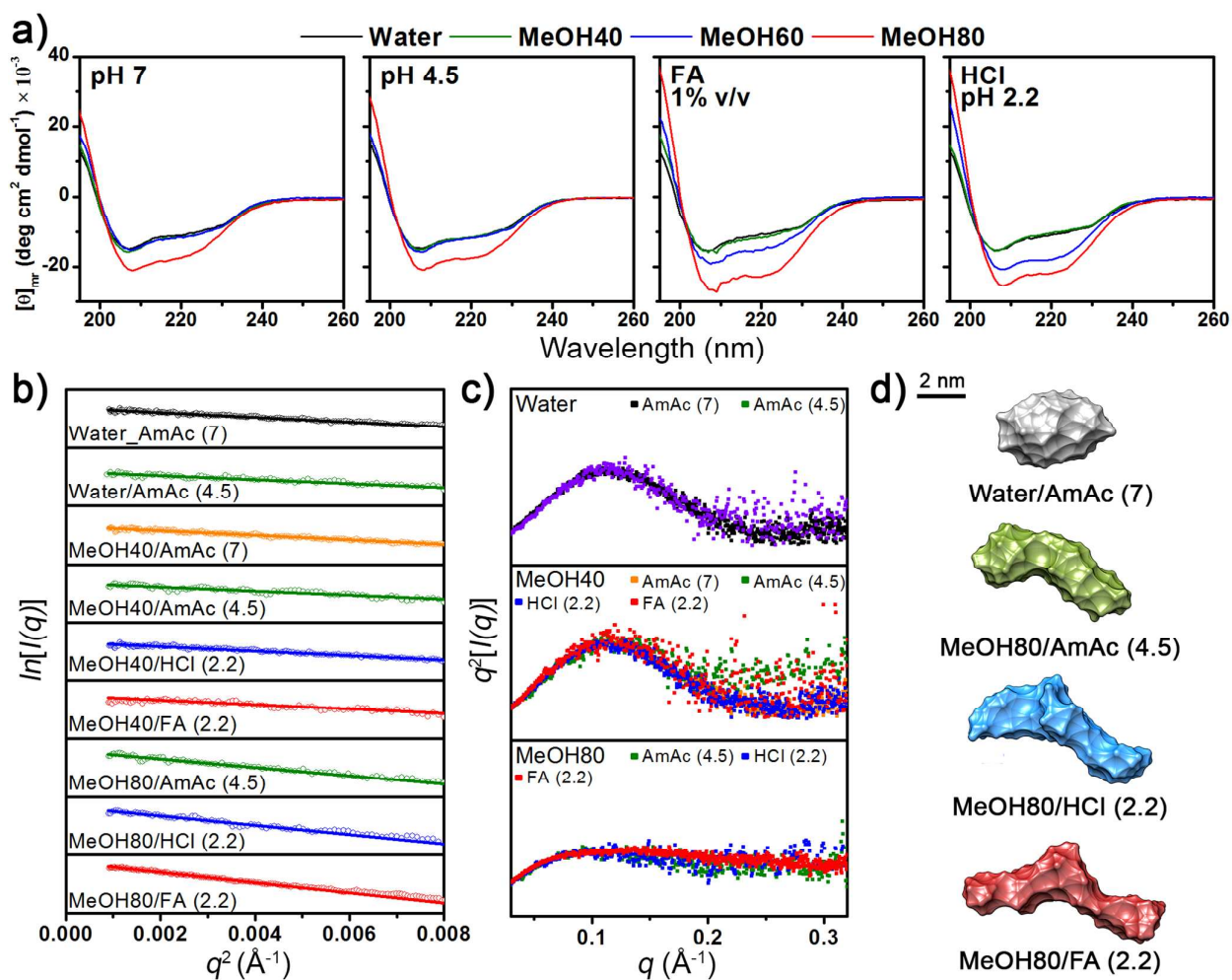


Table 1. R_g and R^2 values,^a and folding states^b of Lyz.

Solution (pH)	$R_g / \text{\AA}$	R^2	Folding State
Water/AmAc ^c (7)	15.3	0.97	Globular
Water (4.5)	14.3	0.92	Globular
MeOH40/AmAc (7)	15.4	0.96	Globular
MeOH40/AmAc (4.5)	14.5	0.87	Globular
MeOH40/HCl (2.2)	15.2	0.96	Globular
MeOH40/FA ^d (2.2)	15.3	0.87	Globular
MeOH80/AmAc (4.5)	20.7	0.87	Unfolded
MeOH80/HCl (2.2)	21.9	0.91	Unfolded
MeOH80/FA (2.2)	22.9	0.98	Unfolded

^a Obtained from linear fitting curves of Guinier plots (Figure 1b), ^b obtained from Kratky plots (Figure 1c), ^c AmAc: ammonium acetate, ^d formic acid.

Figure 2. ESI-MS spectra of Lyz in pure water and 80% methanol (MeOH) solutions without acid, or containing HCl or formic acid (FA).

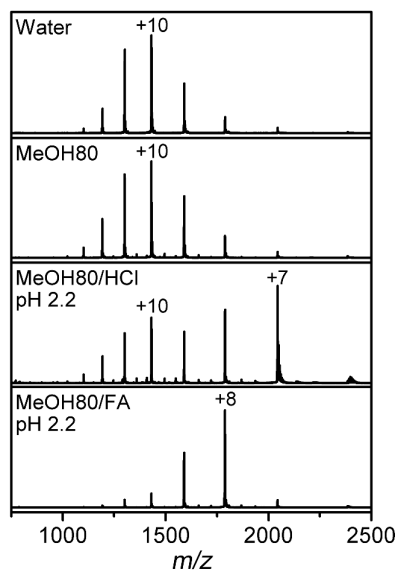
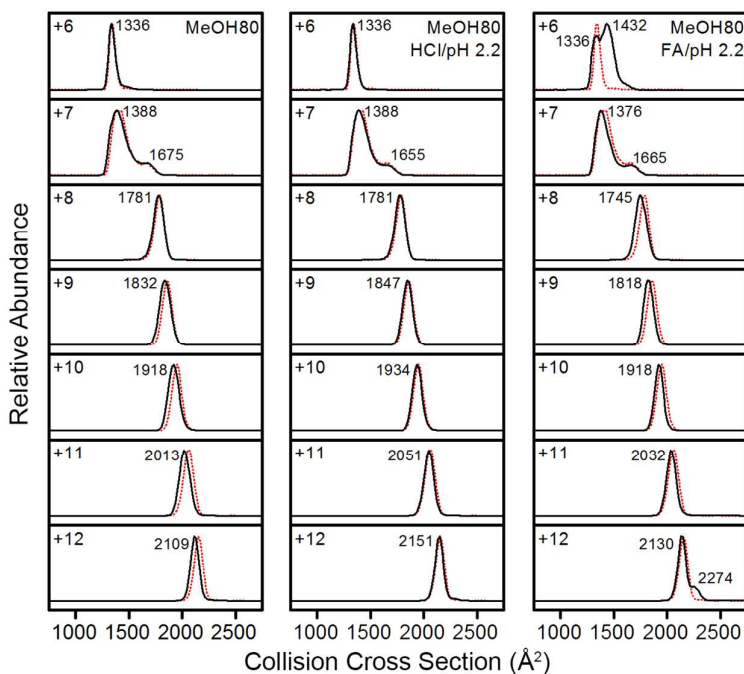
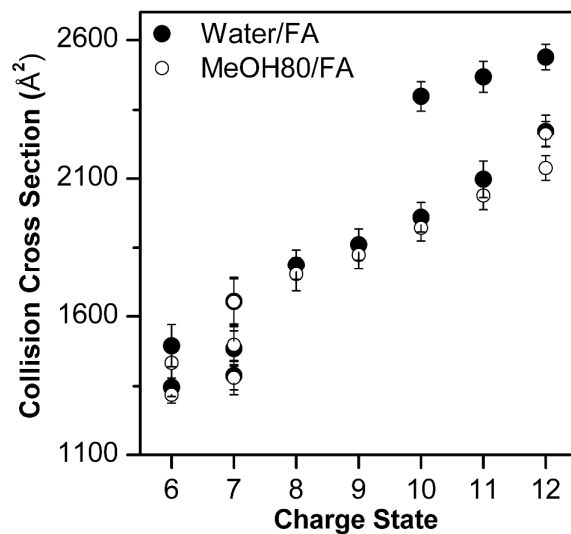


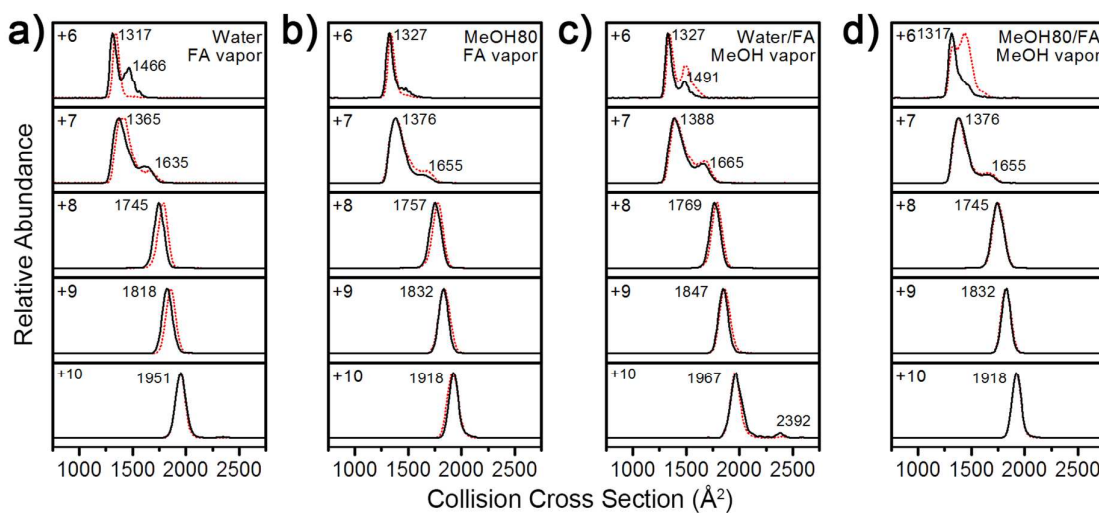
Figure 3. IM spectra of +6 to +12 charged Lyz ions from 80% methanol solutions (black lines). IM spectra of Lyz ions from pure water are given as red dotted lines for comparison.



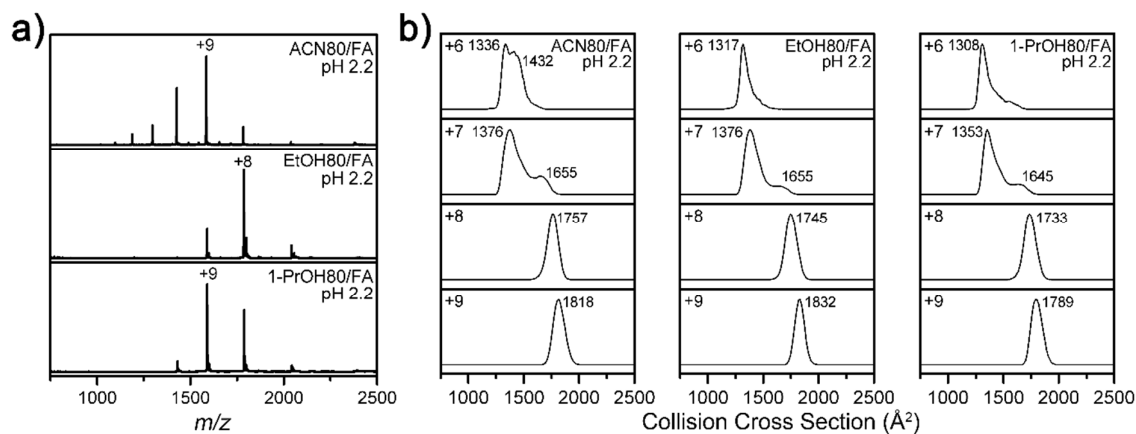
1
2
3
4 **Figure 4.** Comparison between Lyz conformers observed in water/formic acid solution and
5
6 80% methanol/formic acid solution, at pH 2.2. The error bars represent half width at half
7
8 maximum.
9

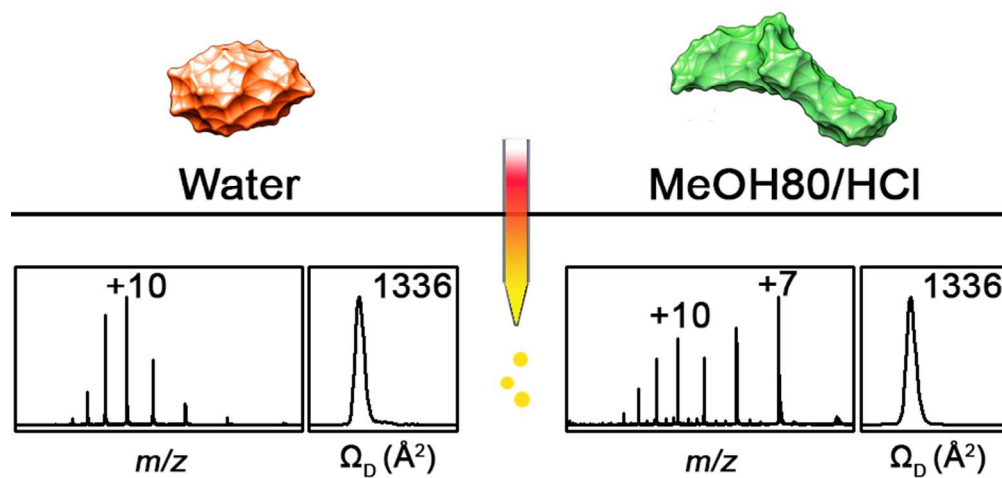


10
11
12
13
14
15
16
17
18
19
20
21
22
23
24
25
26
27
28
29 **Figure 5.** IM spectra of +6 to +10 charged Lyz ions from a) water, exposed to formic acid
30
31 vapor, b) 80% methanol, exposed to formic acid vapor, c) water with formic acid, exposed to
32
33 methanol vapor, and d) 80% methanol with formic acid, exposed to methanol vapor during
34
35 ESI (black lines). IM spectra in the absence of vapor are given as red dotted lines for
36
37 comparison.
38
39



1
2
3
4 **Figure 6.** a) ESI-MS spectra of Lyz in 80% acetonitrile (ACN), ethanol (EtOH), and 1-
5 propanol (1-PrOH) solutions with formic acid, at pH 2.2. b) IM spectra of Lyz ions from 80%
6 ACN, EtOH, and 1-PrOH solutions with formic acid, at pH 2.2.
7
8
9





Organic solvents and acids denature lysozyme in solution. However, they cooperate during ESI to promote its compaction.

80x39mm (300 x 300 DPI)